# Evidence for Helical Edge Modes in Inverted InAs/GaSb Quantum Wells

Ivan Knez and Rui-Rui Du
*Department of Physics and Astronomy, Rice University, Houston, Texas 77251-1892, USA*

Gerard Sullivan
*Teledyne Scientific and Imaging, Thousand Oaks, California 91630, USA*

(Received 29 April 2011; published 19 September 2011)

We present an experimental study of low temperature electronic transport in the hybridization gap of inverted InAs/GaSb composite quantum wells. An electrostatic gate is used to push the Fermi level into the gap regime, where the conductance as a function of sample length and width is measured. Our analysis shows strong evidence for the existence of helical edge modes proposed by Liu *et al* [Phys. Rev. Lett. **100**, 236601 (2008)]. Edge modes persist in spite of sizable bulk conduction and show only a weak magnetic field dependence—a direct consequence of a gap opening away from the zone center.

DOI: 10.1103/PhysRevLett.107.136603 PACS numbers: 72.25.Dc, 73.63.Hs, 73.23.−b

Topological insulators (TI) are a novel phase of matter [1,2], originally predicted to manifest in 2D structures [3] as a superposition of two quantum Hall systems [4], where the role of the spin-dependent magnetic field is played by the spin-orbital interactions. In an extension of the paradigm to 3D, TI surfaces emerge as quarter-graphene with an odd number of Dirac cones [5]. In 2D, the TI phase is also known as a quantum spin Hall insulator (QSHI) and is characterized by an energy gap in the bulk and topologically protected helical edge states. Quantized conductance, taken as the evidence for the QSHI phase, has been experimentally observed in the inverted HgTe/CdTe quantum wells (QWs) [6,7]. Liu *et al* [8] have proposed that QSHI should arise in another semiconductor system, the hybridized InAs/GaSb QWs, where a rich phase diagram including a band insulator and QSHI can be continuously tuned via gate voltages. Here, we present a systematic transport study of high quality InAs/GaSb devices tuned into the QSHI state, where we observe slowly propagating helical edge modes that are largely immune to a conductive bulk. Exploring this system should have a far-reaching impact, since InAs makes a good interface with superconductors [9], a prerequisite for fabricating TI/superconductor hybrid structures [10]; the latter are predicted to host exotic Majorana fermion modes and are viable for fault-tolerant quantum computing.

A common characteristic to all TIs is band inversion, which in InAs/GaSb is achieved by tuning energy levels in two neighboring electron and hole QWs. Hybridization of electron-hole bands leads to a gap opening, which has been experimentally well established, albeit always with a nonzero residual conductivity [11,12]. In an early theoretical study [13], the origin of the residual conductivity has been ascribed to the level-broadening due to scattering. Interestingly, in the ''clean limit,'' the gap conductivity is finite, yet independent of scattering parameters, such as sample mobility. Motivated by the QSHI proposal [8], Knez *et al* [14] revisited the issue of gap conduction in micro-size samples of 15 nm InAs/8 nm GaSb QWs. They found a bulk conductivity $\gtrsim 10e^2/h$ consistent with [13] and a few times larger than the expected contribution from the edge. Nevertheless, bulk conductivity diminishes as the band inversion is reduced [14], promoting the QSHI. Experimentally, this can be readily realized using narrower QWs. In this Letter, we study the length and width dependence of conductance in such QWs in the hybridization regime and find direct evidence for the existence of helical edge modes proposed by Liu *et al.* [8]. Edge modes persist alongside the conductive bulk and show only weak magnetic field dependence. This apparent decoupling between the edge and bulk is a direct consequence of the gap opening away from the zone center, which leads to a large disparity in Fermi wave vectors between bulk and edge states, and results in a qualitatively different QSHI phase than in HgTe/CdTe, where the gap opens at the zone center.

InAs/GaSb has a broken gap band alignment that allows for the coexistence of closely separated electron (in InAs) and hole (in GaSb) two-dimensional gases and is confined by neighboring AlSb barriers, as shown in Fig. 1(a) [15]. For wider wells, the band structure is inverted, i.e., the ground conduction subband ($E1$) is lower than the ground heavy-hole subband ($H1$). The relative position of the $E1$ and $H1$ bands can be tuned by an external electric field [15] applied via the front and back gates. In the inverted regime, the $E1$ and $H1$ bands anticross for some finite wave vector $k_{\mathrm{cross}}$, where electron and hole densities are approximately matched, $n = p = k_{\mathrm{cross}}^2/2\pi$. Because of the tunneling between the wells, electron and hole states are mixed and a hybridization gap opens in the otherwise semimetallic band dispersion, as shown in Fig. 1(b) [15]. The matching of the inverted bands to the corresponding vacuum states leads to an inevitable gap closing at the sample perimeter and results in linearly dispersing edge modes [8]. The time

 

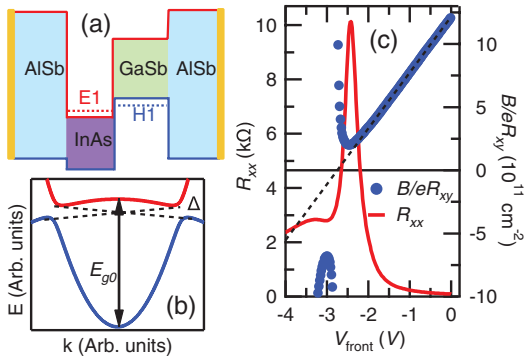


FIG. 1 (color). Panel (a) shows the energy spectrum of inverted CQW, while the band dispersion with linearly dispersing helical edges is shown in panel (b). Panel (c) shows longitudinal resistance $R_{xx}$ (in red) at $B = 0$ T and $B/eR_{xy}$ (in blue), taken at $B = 1$ T, vs the front gate bias $V_{\text{front}}$ for the 50 $\mu$m $\times$ 100 $\mu$m device. As $E_F$ is pushed into the hybridization gap, $R_{xx}$ exhibits a strong peak, concomitantly $B/eR_{xy}$ becomes nonlinear, signaling the two-carrier transport and mini-gap entry.

reversal symmetry of the governing Hamiltonian requires the edge modes to be helical, i.e., counter-propagating spin-up and spin-down channels with conserved helicity. As a result, particles on time-reversed paths around a nonmagnetic impurity in the helical edge destructively interfere, resulting in a zero backscattering probability [2]. For Fermi energy $E_F$ in the gap, the expected edge conductance in a six-terminal configuration for mesoscopic samples will be $2e^2/h$ [7]. Here we use a four-terminal configuration where the expected edge conductance is doubled to $4e^2/h$.

Longer samples can be modeled by inserting phase breaking probes [16] and applying the Landauer-Buttiker formula yielding four-terminal conductance as

$$G_{14,23} = \frac{2e^2}{h}\left[\frac{l_\phi}{L} + \left(\frac{l_\phi}{L}\right)^2\right], \qquad (1)$$

where $l_\phi$ is the phase coherence length and $L$ is the device length. Thus, for macroscopic QSH samples ($L \gg l_\phi$) the edge contribution to the conductance will be negligible. Note that due to the level broadening $\Gamma$ the hybridization gap exhibits a sizable bulk conductivity, which, for small level broadening $\Gamma \ll \Delta$, scales as $g_{\text{bulk}} \sim \frac{e^2}{h}\frac{E_{g0}}{\Delta}$ [13,14], where $E_{g0}$ is the relative separation between $H1$ and $E1$ bands. While the helical edge transport manifests itself only in the mesoscopic regime, macroscopic samples can be used as an important diagnostic of bulk gap conduction, allowing us to separate the edge from bulk contributions which coexist in mesoscopic samples.

The experiments are performed on high quality 12.5 nm InAs/5 nm GaSb quantum wells, in the inverted regime. Sample fabrication and measurement details are given in Refs. [14,17]. Here the data were taken from eight devices made from the same wafer. Figure 1(c) shows longitudinal resistance $R_{xx}$ (in red) vs the front gate bias $V_{\text{front}}$ of a Hall bar with width $W = 50$ $\mu$m and length $L = 100$ $\mu$m, at $B = 0$ T, $T = 300$ mK. As $V_{\text{front}}$ is swept from 0 to $-4$ V, $E_F$ is pushed from a purely electron to a two-carrier hole-dominated regime. When $n \sim p$, a strong resistance peak of $R_{\max} \sim 10.2$ k$\Omega$ is observed, which for this macroscopic sample reflects only the bulk transport, with a bulk gap conductivity of $g_{\text{bulk}} = \frac{\square}{R_{\max}} = 5.05e^2/h$, where $\square = L/W = 2$. Entry into the hybridization gap is also signaled by nonlinearity in $B/eR_{xy}$ (taken at $B = 1$ T), shown in Fig. 1(c) in blue. Negative values of $B/eR_{xy}$ indicate a hole-dominated regime although in the two-carrier regime direct correspondence to the carrier density no longer exists. The size of the mini gap can be determined from the relative position in $V_{\text{front}}$ of the resistance dip, which corresponds to the van Hove singularity at the gap edge, and the resistance peak which corresponds to the middle of the gap [11,14]: $\Delta = 2(V_{\text{peak}} - V_{\text{dip}})\frac{\Delta n}{\Delta V}\frac{1}{\text{DOS}}$, where $\frac{\Delta n}{\Delta V} = 4.2 \times 10^{11}$ cm$^{-2}$/V is the rate of carrier density change with $V_{\text{front}}$ and DOS $= (m_e + m_h)/\pi\hbar^2$ is the density of states, with carrier masses $m_e = 0.03$ and $m_h = 0.37$ (in units of free electron mass), [11] giving $\Delta \sim 4$ meV. From the minimum in $B/eR_{xy}$, which corresponds to an anticrossing density of $n_{\text{cross}} \sim 2 \times 10^{11}$ cm$^{-2}$, we can estimate $E_{g0} = n_{\text{cross}}\frac{\pi\hbar^2}{m^*} \sim 16$ meV, where $m^*$ is the reduced mass. The expected bulk conductivity is then [13] $g_{\text{bulk}} \sim \frac{e^2}{h}\frac{E_{g0}}{\Delta} \sim \frac{4e^2}{h}$, consistent with the observed value.

Figure 2(a) shows resistance peaks for $L = 100, 10, 4,$ and 2 $\mu$m, with $\square = 2$. The resistance peak of the $L = 100$ $\mu$m device is used to estimate the bulk gap resistance $R_{\text{bulk}} \sim 10.2$ k$\Omega$. A parallel combination of $R_{\text{bulk}}$ and the expected edge resistance $h/4e^2$, gives a resistance value of $R_{\text{bulk}} \| h/4e^2 \sim 3.95$ k$\Omega$ [dashed black line in Fig. 2(a)], which is just slightly above the measured valued of $R_{\max} \sim 3.75$ k$\Omega$ for the $L = 2$ $\mu$m device. A plot of the gap conductance $G$ vs $1/L$ in Fig. 2(b) can be fitted with Eq. (1), obtaining $l_\phi = (2.07 \pm 0.25)$ $\mu$m and giving further evidence for the existence of helical edge conduction channels in mesoscopic samples. In fact, the difference in conductance between the mesoscopic and the macroscopic samples is just slightly above $4e^2/h$, as expected for helical edge modes [18].

In a width dependence experiment, we fix $L = 2$ $\mu$m, while $W$ is varied from $W = 0.5, 1, 1.5,$ to 2 $\mu$m. While the resistance peaks shown in Fig. 2(c) increase as $W$ is decreased, the plot of $G$ vs $W$ in Fig. 2(d) reveals a reasonably linear relationship with an intercept of the linear fit of $G_{\text{edge}} = (4.08 \pm 0.69)\frac{e^2}{h}$, in support of helical edge transport. As an important check, the slope of the same fit gives a bulk conductivity of $g_{\text{bulk}} = (5.46 \pm 1.01)\frac{e^2}{h}$, which is consistent with the value estimated earlier. Thus, both the length and the width dependence of the gap

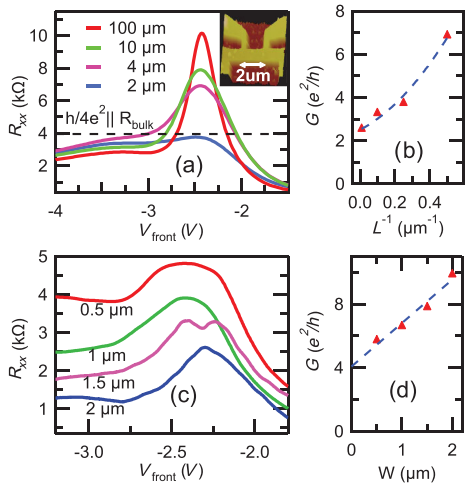


FIG. 2 (color). Panel (a) shows $R_{xx}$ vs $V_{\text{front}}$ for devices with $L = 100, 10, 4$, and 2 $\mu$m (AFM image in inset) while $W$ is varied to give a constant geometric factor $\square = L/W = 2$; $B = 0$ T, $T = 300$ mK. Resistance peaks decrease for shorter devices and approach the limit $R_{\text{bulk}} \| h/4e^2$ (dashed line) for the 2 $\mu$m device. Panel (b) shows gap conductance $G$ vs $L^{-1}$ and is fitted with Eq. (1) (dashed line) giving coherence length $l_\phi = 2.07 \pm 0.25$ $\mu$m. The conductance difference between the mesoscopic and macroscopic device is $\sim 4e^2/h$ suggestive of helical edge transport. Panel (c) shows $R_{xx}$ vs $V_{\text{front}}$ for devices with $W = 0.5, 1, 1.5$, and 2 $\mu$m; $L = 2$ $\mu$m. Resistance peaks decrease with increasing $W$. The gap conductance $G$ vs $W$ in panel (d) shows a linear relationship. The intercept of the linear fit is $G_{\text{edge}} = (4.08 \pm 0.69)\frac{e^2}{h}$, as expected for the helical edge transport, while the slope of the fit gives bulk conductivity $g_{\text{bulk}} = (5.46 \pm 1.01)\frac{e^2}{h}$ [consistent with data in (a)].

conductance consistently confirm the existence of helical edge channels in inverted InAs/GaSb QWs.

Using $V_{\text{back}}$ the anticrossing point $k_{\text{cross}}$ can be tuned to lower values, thereby suppressing $g_{\text{bulk}}$. Figure 3 shows $R_{xx}$ vs $V_{\text{front}}$ with $V_{\text{back}}$ varied in 2 V steps from 0 to $-8$ V for devices of $L = 100$ $\mu$m in (a), $L = 2$ $\mu$m in (b), and $\square = 2$ in both cases. As $V_{\text{back}}$ is tuned to more negative values, the separation between the bands $E_{g0}$ is reduced, and the resistance peaks of the $L = 100$ $\mu$m sample increase from $R_{\text{max}} \sim 10$ k$\Omega$ at $V_{\text{back}} = 0$ V, to $R_{\text{max}} \sim 50$ k$\Omega$ at $V_{\text{back}} = -8$ V. On the other hand, the resistance peaks of the mesoscopic sample increase only slightly, from $R_{\text{max}} \sim 4$ k$\Omega$ at $V_{\text{back}} = 0$ V, to $R_{\text{max}} \sim 6$ k$\Omega$ at $V_{\text{back}} = -8$ V. In fact, the conductance difference between mesoscopic and macroscopic samples, $\Delta G = G_{2\,\mu\text{m}} - G_{100\,\mu\text{m}}$, stays around $\sim 4e^2/h$ for all values of $V_{\text{back}}$, as shown in Fig. 3(c), accounting for the helical edge transport.

Data presented in Fig. 3(a) may suggest that edge conduction is completely independent of gap bulk conductivity, $g_{\text{bulk}}$. However, this is valid only in the regime of low $g_{\text{bulk}}$. Note that in Fig. 3(a) $g_{\text{bulk}} \lesssim 5e^2/h$. Using the bias cooling technique [14], the system can be pushed deeper into the inverted regime, i.e., a larger $E_{g0}$ can be obtained, so that at $V_{\text{back}} = 0$ V, $g_{\text{bulk}} \sim 19e^2/h$, while at $V_{\text{back}} = -8$ V,

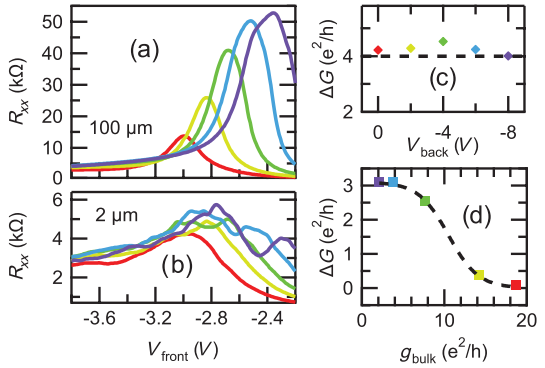


FIG. 3 (color). Panel (a) shows $R_{xx}$ vs $V_{\text{front}}$ for devices with $L = 100$ $\mu$m, and in (b) for $L = 2$ $\mu$m with $V_{\text{back}}$ varied in 2 V steps from 0 to $-8$ V; $\square = 2$, $B = 0$ T, $T = 20$ mK. As $V_{\text{back}}$ is tuned to more negative values, the mini-gap moves to smaller wave vectors and the resistance peaks increase. The difference in gap conductance between the 2 and 100 $\mu$m sample, $\Delta G$ vs $V_{\text{back}}$, is shown in (c), with $\Delta G \sim 4e^2/h$ for all values of $V_{\text{back}}$. Note that $g_{\text{bulk}} \lesssim 5e^2/h$. Panel (d) shows $\Delta G$ vs $g_{\text{bulk}}$ for a bias cooled sample with a larger bulk conduction. Edge conduction "activates" for $g_{\text{bulk}} \lesssim 10e^2/h$.

$g_{\text{bulk}} \sim e^2/h$. In this case, the edge conductance, i.e., $\Delta G = G_{2\,\mu\text{m}} - G_{100\,\mu\text{m}}$, goes from $\Delta G \sim 0$ for the large bulk conductivity of $g_{\text{bulk}} \sim 19e^2/h$ to about $\Delta G \sim 3e^2/h$ as the bulk conductivity is reduced to $g_{\text{bulk}} \lesssim 5e^2/h$, as shown in Fig. 3(d). The cutoff bulk conductivity at which edge conduction "activates" can be estimated to $g_{\text{bulk}} \sim 10e^2/h$.

The apparent resilience of edge conduction to bulk transport is quite unexpected, considering that a conductive bulk would allow edge electrons to tunnel from one side to another, resulting in interedge scattering and a reduced edge conductance [19,20]. However, the interedge tunneling probability may be significantly reduced by a large Fermi wave vector mismatch. The bulk gap states are inherited from the nonhybridized band structure and have a Fermi wave vector equal to $k_{\text{cross}} \gg 0$ while edge modes, for $E_F$ situated in the middle of the gap, have $k_{\text{edge}} \sim 0$. Thus, due to $k_{\text{edge}} \ll k_{\text{cross}}$, edge modes are totally reflected from bulk states. In fact, the tunneling probability for the edge electrons will be proportional to the edge-bulk transmission probability, which scales as $k_{\text{edge}}/k_{\text{cross}}$, as well as the bulk transmission, which scales as bulk conductivity, i.e., as $Ego \propto k_{\text{cross}}^2$. Hence, the overall interedge tunneling probability will decrease as $k_{\text{cross}}$ is reduced, which is in a qualitative agreement with the data in Fig. 3(d). Furthermore, due to the low Fermi velocity of edge states $v = \frac{1}{\hbar}\frac{\partial E}{\partial k} \sim \frac{1}{\hbar}\frac{\Delta}{2k_{\text{cross}}} \sim 3 \times 10^4$ m/s, relativistic effects of the Rashba spin-orbital interaction will be small, and electron spins are expected to be aligned along the growth axis, reducing interedge tunneling due to the Pauli exclusion [21].

The resistance peaks of mesoscopic samples show only a weak dependence on in-plane and perpendicular magnetic

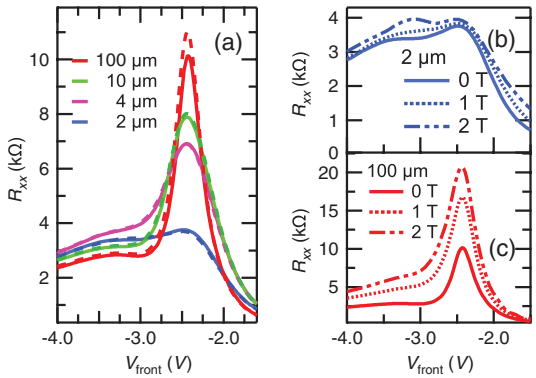


FIG. 4 (color). Panel (a) shows $R_{xx}$ vs $V_{\text{front}}$ at the in-plane field $B_{\parallel} = 0$ T (full line) and $B_{\parallel} = 1$ T (dashed line) for $L =$ 100, 10, 4, and 2 $\mu$m, indicating a weak field dependence of the gap resistance; $T = 300$ mK. Panel (b) shows $R_{xx}$ vs $V_{\text{front}}$ at perpendicular fields of $B_{\text{perpen}} = 0$ T, 1 T, and 2 T for $L = 2$ $\mu$m, and in panel (c) for $L = 100$ $\mu$m.

fields, as shown in Figs. 4(a) and 4(b), respectively, while macroscopic samples show a much stronger dependence. At first glance, this appears to be in contrast to the strong field dependence reported for HgTe/CdTe QWs [7]. However, even in HgTe a strong magnetic field dependence has never been observed in the smallest micron size samples [21], but only in longer (20 $\mu$m) samples [7]. In fact, it has been shown theoretically by Maciejko *et al* [22] that the magnetic field decay of edge modes depends sensitively on disorder strength. In particular, pronounced cusplike features in magnetoconductance can occur when the disorder strength is larger than the gap. In this limit, electrons can diffuse into the bulk, enclosing larger amounts of flux whose accumulation destroys destructive interference of backscattering paths, resulting in a linear decay of conductance with $B$. In the case of HgTe, the large disorder was provided by inhomogenous gating, which is more pronounced for longer devices [7].

In InAs/GaSb, edge states are effectively decoupled from the bulk and the above flux effect plays a lesser role, resulting in a weaker magnetic field dependence of edge modes. However, the decay of bulk conductivity itself, with a magnetic field, may not necessarily be weak due to the localization of nonhybridized carriers. This localization is more pronounced for longer samples, which have stronger disorder. Thus, longer samples are expected to show stronger magnetic field dependence, as experimentally observed. We note here that localization at high magnetic fields results in a dramatic reentrant quantum Hall effect [17]. Such reentrant behavior is a signature mark of topologically distinct band structure [7], and its observation validates the topological origin of helical edge modes at the zero magnetic field.

In conclusion, inverted InAs/GaSb CQWs in a hybridization regime host slowly propagating helical edge modes, which persist despite their conductive bulk and show only weak magnetic field dependence. This remarkable property can be qualitatively explained by a gap opening away from the Brillouin zone center, unlike in HgTe where the gap opens at $k \sim 0$. Demonstrated band structure tunability and good interface to superconductors make this QSHI system a promising candidate in the realization of exotic Majorana modes.

The work at Rice was supported by the Rice Faculty Initiative Fund, Hackerman Advanced Research Program Grant No. 003604-0062-2009, Welch Foundation Grant No. C-1682, and NSF Grant No. DMR-0706634. I. K. acknowledges financial support from the M. W. Keck Foundation. We thank S.-C. Zhang for bringing our attention to Ref. [8], S.-C. Zhang, X.-L. Qi, C. Liu, J. Maciejko, and M. Konig for many helpful discussions.

[1] M. Z. Hasan and C. L. Kane, Rev. Mod. Phys. **82**, 3045 (2010).
[2] X.-L. Qi and S.-C. Zhang, [arXiv:1008.2026 [Rev. Mod. Phys. (to be published)].
[3] C. L. Kane and E. J. Mele, Phys. Rev. Lett. **95**, 226801 (2005).
[4] B. A. Bernevig, S. C. Zhang, Phys. Rev. Lett. **96**, 106802 (2006).
[5] L. Fu, C. L. Kane, and E. J. Mele, Phys. Rev. Lett. **98**, 106803 (2007).
[6] B. A. Bernevig, T. L. Hughes, and S.-C. Zhang, Science **314**, 1757 (2006).
[7] M. Konig, S. Wiedmann, C. Brune, A. Roth, H. Buhmann, L. W. Molenkamp, X.-L. Qi, and S.-C. Zhang, Science **318**, 766 (2007).
[8] C. Liu, T. L. Hughes, X.-L. Qi, K. Wang, and S.-C. Zhang, Phys. Rev. Lett., **100**, 236601 (2008).
[9] C. Nguyen, J. Werking, H. Kroemer, and E. L. Hu, Appl. Phys. Lett. **57**, 87 (1990).
[10] L. Fu, and C. L. Kane, Phys. Rev. Lett. **100**, 096407 (2008).
[11] M. J. Yang, C. H. Yang, B. R. Bennett, and B. V. Shanabrook, Phys. Rev. Lett. **78**, 4613 (1997).
[12] L. J. Cooper, N. K. Patel, V. Drouot, E. H. Linfield, D. A. Ritchie, and M. Pepper, Phys. Rev. B **57**, 11915 (1998).
[13] Y. Naveh and B. Laikhtman, Europhys. Lett. **55**, 545 (2001).
[14] I. Knez, R. R. Du, and G. Sullivan, Phys. Rev. B **81**, 201301(R) (2010).
[15] Y. Naveh and B. Laikhtman, Appl. Phys. Lett. **66**, 1980 (1995).
[16] See, e.g., S. Datta, *Electronic Transport in Mesoscopic Systems* (Cambridge University Press, Cambridge, 1995).
[17] I. Knez, R. R. Du, and G. Sullivan (to be published).
[18] The small difference may come from a logarithmic correction to bulk conductivity due to localization which goes as $\Delta g = -\frac{e^2}{\pi h}\text{Ln}(\frac{L}{l})$, where $l$ is the mean free path. See, e.g., E. Abrahams, P. W. Anderson, D. C. Licciardello, and T. V. Ramakrishnan, Phys. Rev. Lett. **42**, 673 (1979). However, the logarithmic correction accounts only

for the fraction of the difference in conductance between mesocopic and macroscopic samples, i.e., $\Delta G = \frac{e^2}{\square \pi h} \mathrm{Ln}(\frac{100\ \mu\mathrm{m}}{2\ \mu\mathrm{m}}) \sim 0.6\frac{e^2}{h}$ compared to a total difference of $\gtrsim 4e^2/h$.

[19] B. Zhou, H.-Z. Lu, R.-L Chu, S.-Q. Shen, and Q. Niu, Phys. Rev. Lett. **101**, 246807 (2008).

[20] J. I. Väyrynen and T. Ojanen, Phys. Rev. Lett. **106**, 076803 (2011).

[21] M. Konig, Ph.D. thesis, Wurzburg University, 2007; (private communications).

[22] J. Maciejko, X.-L. Qi, and S.-C. Zhang, Phys. Rev. B **82**, 155310 (2010).